Three-dimensional model of a muscle and simulation of its surface EMG

M.-A. Schnetzer[1,2], D. G. Rüegg[2], R. Baltensperger[1], J.-P. Gabriel[1]

[1]Department of Mathematics, University of Fribourg, Switzerland

[2] Department of Medicine, University of Fribourg, Switzerland

Abstract- **The aim of this paper was to present a spatial model of a muscle including all its motor units (MU) and a simulation of its surface EMG. The simulations are part of a larger model including in addition the input system to the motoneuronal pool, the motoneuronal pool itself and the force generating mechanism. The muscle and the MU territories are represented by elliptic cylinders. Two algorithms are presented to position the MU territories within the muscle. The final goal was to achieve a final global fiber density, which is as constant as possible. The algorithm, which minimizes the variability of the fiber density each time a MU territory is positioned, proved to be superior. The surface EMG of this model muscle was simulated by assuming that each muscle fiber generates an action potential (AP) at the motor endplate in the middle of the fiber and propagates it at constant velocity to both ends. APs were represented by a tripole and the sum of the potentials evoked by the tripoles generates a fiber AP at the recording site. All the fibers within the MU territory generate the MU AP and finally all active MUs together give rise to the surface EMG. As example, the steady activity of the human first dorsal interosseus muscle was simulated. The surface EMGs, recorded with an array of electrodes around and along the muscle, were illustrated.**

I. Introduction

A skeletal muscle is composed of muscle fibers grouped in motor units (MUs). The number of MUs in mammalian muscles ranges from ten to several thousands and each one consists of a motoneuron (MN) together with the muscle fibers under its control. During most voluntary and reflex contractions, MUs are recruited during force increase according to their tetanic contraction force (size principle [1,2]) and recruited MUs enhance their force by frequency modulation. The activity of a muscle can be recorded with the surface electromyogram (EMG), a tool used extensively in neurological clinics and research. The aim of this study was to develop a model of the MU pool, its geometry and the surface EMG evoked by its active MUs.

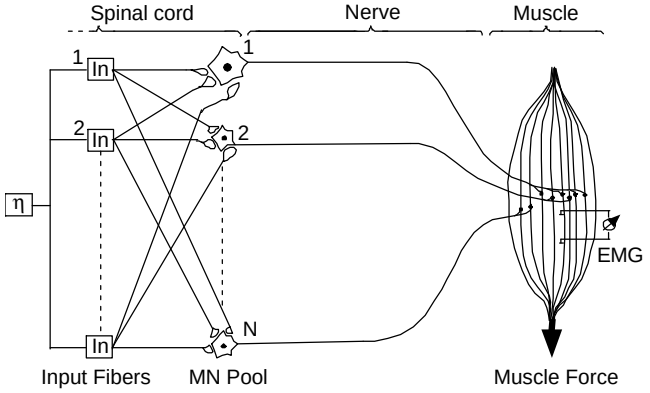

Fig. 1. Model of the MN pool-muscle complex. A time-dependent variable η (activation factor) controls the activity of the *N* MNs which activate the muscle fibers of the corresponding MUs.

II. The Model

The present work is part of a larger model of the whole MN pool-muscle complex, which includes: (1) the input to the MN pool, (2) the MN pool, (3) the force generating mechanism, (4) a spatial model of the muscle, and (5) the surface EMG (Fig. 1). Part (1), (2) and (3) can be found in [3] whereas part (4) and (5) are the object of the present paper.

A. The MU distribution

The MUs are characterized by their tetanic contraction force. As described in [3] and [4], the (continuous) distribution of the MU population ρ as a function of the MU tetanic contraction force τ is assumed to be exponential:

$$r(t) = a\exp(-bt)\,, \tag{1}$$

where *a* and *b* are muscle dependent constants. This relation is valid for τ between τ_{min} and τ_{max}, the tetanic contraction forces of the smallest resp. largest MU. Given this relation, the number of MUs of the pool and the maximal muscle force can be deduced from ρ. More precisely,

$$N = \int_{t_{min}}^{t_{max}} r(t)\,dt = -\frac{a}{b}\left[\exp(-bt_{max}) - \exp(-bt_{min}\right], \tag{2}$$

and

$$F_{max} = \int_{t_{min}}^{t_{max}} t\,r(t)\,dt\,. \tag{3}$$

F_{max}, the decay constant *b*, the contraction forces of the weakest τ_{min} and of the strongest τ_{max} MUs are supposed to be given. The number of MUs is then obtained by eliminating the constant *a* in (2) and using (3). The tetanic contraction force of the MUs is given by the distribution function (1) where each MU covers an area equal to one under the preceding curve:

$$\int_{t_i}^{t_{i+1}} r(t)\,dt = 1\,,\ i = 1,\ \ldots,\ N\text{-}1, \tag{4}$$

where τ_i is the contraction force of *i*-th MU.

The contraction force of MU *i+1* is

$$t_{i+1} = -\frac{1}{b}\ln\left(\exp(-bt_i) - \frac{b}{a}\right). \tag{5}$$

Report Documentation Page

Report Date	Report Type	Dates Covered (from... to)
25OCT2001	N/A	-

Title and Subtitle Three-dimensional model of a muscle and simulation of its surface EMG	**Contract Number**
	Grant Number
	Program Element Number
Author(s)	**Project Number**
	Task Number
	Work Unit Number
Performing Organization Name(s) and Address(es) Department of Mathematics, University of Fribourg, Switzerland	**Performing Organization Report Number**
Sponsoring/Monitoring Agency Name(s) and Address(es) US Army Research, Development & Standardization Group (UK) PSC 802 Box 15 FPO AE 09499-1500	**Sponsor/Monitor's Acronym(s)**
	Sponsor/Monitor's Report Number(s)

Distribution/Availability Statement
Approved for public release, distribution unlimited

Supplementary Notes
Papers from the 23rd Annual International Conference of the IEEE Engineering in Medicine and Biology Society, October 25-28, 2001, held in Istanbul, Turkey. See also ADM001351 for entire conference on cd-rom., The original document contains color images.

Abstract

Subject Terms

Report Classification unclassified	**Classification of this page** unclassified
Classification of Abstract unclassified	**Limitation of Abstract** UU

Number of Pages
6

Since there are N areas and $N+1$ values τ_i, τ_N and τ_{max} are slightly different. The tetanic force of the last MU is defined to be τ_N. As an example, the MU population of the first dorsal interosseus (FDI) muscle is given in Fig. 2.

B. The Muscle

In its final version, the 3-dimensional model will represent a muscle with an elliptic cross sectional area, with parallel fibers and with an angle α between the direction of the fibers and the action of force (pennation angle). The case with positive α can be recovered by shearing a muscle with α=0 (forthcoming paper).

We consider here a muscle represented by an elliptic cylinder, situated in a 3-dimensional coordinate system, with pennation angle α=0. The motor endplates of the fibers are in their middle and positioned in the horizontal x-y plane.

The fiber diameters within a human muscle do not depend consistently on the fiber or MU type [5,6] and their variability is relatively small; we therefore assume a constant diameter of all the muscle fibers. Like in a real muscle, the fibers of a MU will not be scattered throughout the whole muscle cross sectional area (MCSA) but limited to a region with a rather constant fiber density called MU territory (MUT).

For similar reasons, the fiber density within a MUT is assumed to be constant [7]. A reasonable model for MUTs are ellipses [8, 9] whose axes are parallel to the ones of the MCSA. The ratio e between the major and minor axis of each MUT and of the MCSA is the same. Assuming that all muscle fibers contract with the same force τ_f, the contraction force of the MU i is given by :

$$t_i = MUT_i \, d_i \, t_f \,, \tag{6}$$

where d_i is the density of the fibers of the MU i. Denoting the major semi axis of MUT_i by r_i, we have $MUT_i = \pi \, r_i^2/e$, and

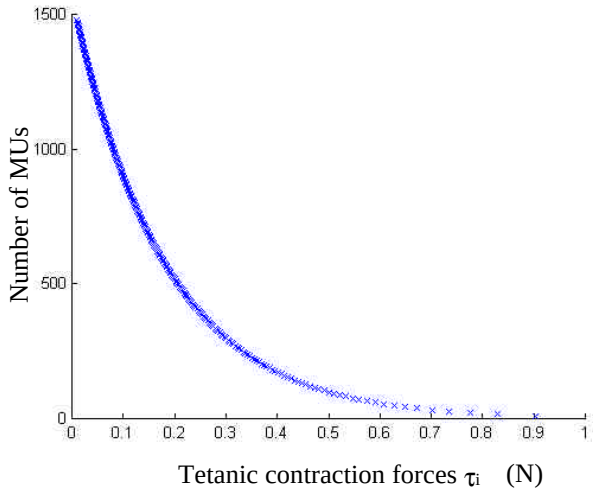

Fig. 2. Exponential distribution of the tetanic contraction force τ_i (N) of the FDI muscle. Forces range between 0.01 N and 1 N. Crosses represent individual MUs.

thus:

$$r_i = \sqrt{\frac{e\,t_i}{p\,t_f\,d_i}} \,. \tag{7}$$

The fiber density is larger in large than in small MUs [10], but the exact relation between the fiber density and the MU size is not known. It seems reasonable to assume a linear relationship between the MU force and the density:

$$d_i = f + g\,t_i \,, \tag{8}$$

where f and g are constants to be determined. By assuming that the fiber density of the smallest MU is m times smaller than the density of the largest one, we get a system of 3 equations for the unknown variables f, g, d_1 and d_N:

$$\begin{cases} d_1 = f + g\,t_1, \\ d_N = f + g\,t_N, \\ d_N = m\,d_1. \end{cases} \tag{9}$$

Using d_1 as a free parameter, f and g can be determined and introduced in (8):

$$d_i = \frac{d_1}{t_N - t_1}\left(t_N - m\,t_1 + (m-1)\,t_i\right). \tag{10}$$

Since the total area of the MUTs is p times larger than the one of the MCSA [11], they have to overlap and according to (6):

$$p\,MCSA = \frac{1}{t_f}\sum_{i=1}^{N}\frac{t_i}{d_i} \,. \tag{11}$$

Replacing d_i in (11) with (10) and solving for d_1, we get

$$d_1 = \frac{(t_N - t_1)}{p\,t_f\,MCSA}\sum_{i=1}^{N}\frac{t_i}{t_N - m\,t_1 + (m-1)\,t_i} \,. \tag{12}$$

d_i and r_i can now be determined from (10) and (7).

C. Location of MUTs

It seems clear that the two following conditions can not be fulfilled simultaneously: (1) each MU has an elliptic MUT with a constant fiber density and (2) the global fiber density is constant throughout the whole MCSA (global fiber density of the MCSA is the sum of the densities of the MUTs overlapping in the regions of interest). We therefore look for configurations of the MUTs for which regional differences of the global fiber density are small. In order to attribute a center to each MUT in the plane of the MCSA, the latter is divided into squares of equal size. In this section, the word "point" will refer indifferently to the point in the center of a square and to the square itself. The global density δ at point j of the muscle is the sum of the densities of the MUTs containing the point $A(j)$:

$$d(j) = \sum_{i \in A(j)} d_i \,, \tag{13}$$

where

$$A(j) = \{i;\, j \in MUT_i\} \,. \tag{14}$$

The MUT distribution within the MCSA is obtained by choosing the MUT according to the algorithms described below. During the positioning process, a MUT may intersect

the muscle boundary. Such a MUT can be adjusted in two different ways so that it does not extend over the muscle boundary and that its center remains unchanged: (1) the external part of the territory is cut off, and the semi axes of the MUT are increased in order to achieve the correct area, (2) the part of the MUT extending over the muscle boundary is cut off, without size adjustment. With the second procedure, the average fiber density within the muscle remains unchanged, whereas the MUT and hence the MU tetanic contraction force are slightly modified. Due to its simplicity, and since we wanted to maintain the fiber density, we chose the second method.

We propose two different algorithms to place the MUTs. In both cases, the global densities at all points are set to 0, and the MUTs are positioned according to decreasing size.

In the first algorithm, all points within the MCSA for which the global density is minimal or approaches the minimal value are determined. One of these points is chosen randomly from a uniform distribution as the center of the MUT to be placed.

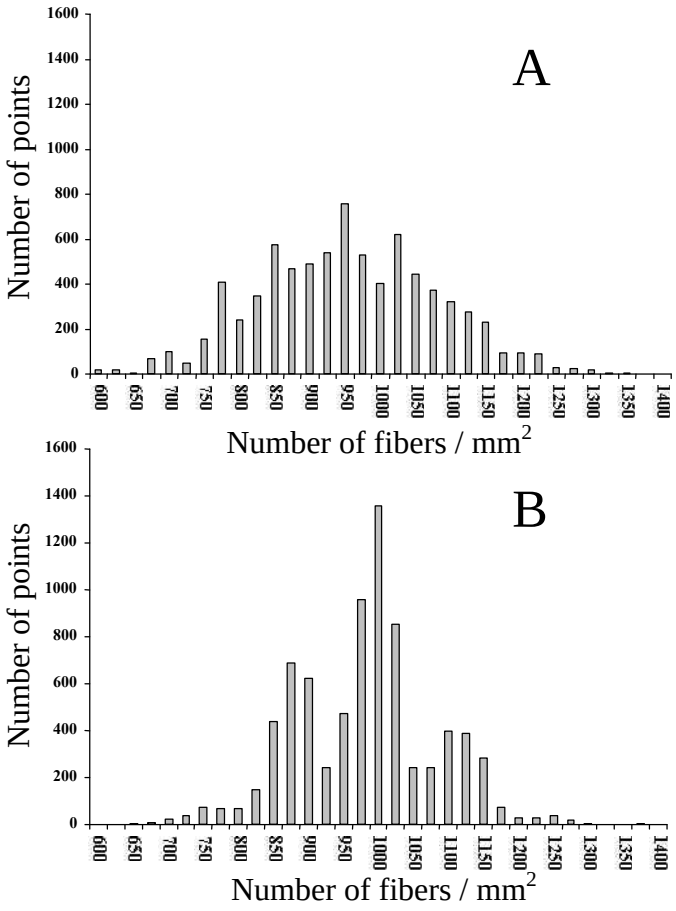

Fig. 3. Distributions of the global densities inside the MCSA of the FDI muscle using algorithm 1 (A) and 2 (B). *X*-axis: point densities; *y*-axis: number of occurrences in a simulation with 10'000 squares. In A, densities range from 464 up to 1634 fibers / mm ^{2}. In B, densities range from 618 up to 1365 fibers / mm ^{2}. Extremely small *y* values are not visible. The vertical range of B is almost twice the one of A.

In the second algorithm, the MUT to be placed is positioned at each point within the MCSA. For each position the variance of the global density is computed. The variance is

$$Var(d) = \frac{1}{n}\sum_{j=1}^{n}(d(j)-\bar{d})^2 , \qquad (15)$$

where n is the total number of points inside the MCSA, $\delta(j)$ is given in (13) and

$$\bar{d} = \frac{1}{n}\sum_{j=1}^{n} d(j) . \qquad (16)$$

The set of points with minimal variance is determined. As in the first algorithm, a point within the set is chosen randomly and becomes the center of the MUT to be positioned. As soon as most of the MCSA is covered by at least one MUT, there is usually only one point achieving the minimal variance.

D. The surface EMG

As already mentioned, each muscle fiber has a motor endplate in its middle. If the endplate is excited, an action potential (AP) is generated at the postsynaptic membrane and propagated with constant velocity in both directions along the muscle fiber. APs are simulated with a tripole consisting of a current source, followed by a sink and by another current source.

A current source I in an unlimited uniform conductor induces a potential Φ at a distance D given by

$$\Phi = \frac{I}{4p\, c\, D} , \qquad (18)$$

where c is the conductivity of the medium.

The conductivity within a muscle is far from being homogeneous since it is about 5 times greater along than perpendicular to the fiber [12]. Correcting for the anisotropy [13], we get

$$\Phi = \frac{I}{4p\, c_r \sqrt{r^2 c_z / c_r + z^2}} , \qquad (19)$$

where r and z are the radial resp. longitudinal distance between point electrode and fiber motor endplate, c_r the radial and c_z the longitudinal conductivity.

Since APs are transmitted from the endplate in both directions, we have to consider 2 current sinks and 4 current sources. At time $t=0$ (generation of the AP), the sinks are positioned at the motor endplate. A fiber AP is thus determined by 4 current sources (I_1, I_3, I_4 and I_6) and 2 current sinks (I_2 and I_5):

$$FAP(r,t) = \frac{1}{4p\, c_r}\sum_{k=1}^{6}\frac{I_k}{D_k(t)} , \qquad (20)$$

where

$$D_k(t) = \sqrt{r^2 c_z / c_r + z_k^2}\ , \qquad (21)$$

and z_k the longitudinal distance between electrode and point k of the tripole.

Taking into account the current intensity by introducing the weighting factors ω_k [14], (20) yields

$$FAP(r,t) = \frac{I}{4p\ c_r} \sum_{k=1}^{6} \frac{w_k}{D_k(t)}, \qquad (22)$$

with $\omega_1 = \omega_4 = 2/3$,
$\omega_2 = \omega_5 = -1$,
$\omega_3 = \omega_6 = 1/3$.

When approaching the end of the fiber, the currents were decided to decrease linearly and vanish ultimately.

A MU AP (MUAP) is defined as the sum of the potentials evoked by all the fibers of a MU. In order to approximate quantitatively a MUAP, the MUT is subdivided in equidistant grid points whose distance can be controlled by the user. For each fiber passing through such a point, the corresponding fiber AP is computed and the potentials at all points within the MUT are added. Let us recall that the tetanic contraction force τ_i divided by the (constant) force of a single muscle fiber τ_f provides the total number of fibers of the MU *i*. An approximation of the MUAP is hence given by multiplying the preceding sum with the quotient M_i/C_i, where M_i is the number of fibers of the MU *i* and C_i the number of grid points in the MUT *i*. We thus get:

$$MUAP_i(t) = \frac{M_i}{C_i} \sum_{(x,y)\in MUT_i} FAP(r,t)\ , \qquad (23)$$

for $t > 0$.

Adding the MUAPs of the active MUs relative to the beginning of the EMG recording ($t=0$), we obtain the surface EMG at time t :

$$EMG(t) = \sum_i \sum_j MUAP_i(t - t_{ij})\ , \qquad (24)$$

where t_{ij} is the time of occurrence of the j-th AP of the MU i.

The activity of the MUs is provided by another part of the model of the motoneuron pool muscle complex [3]. The input to the model is given by a time-dependent activation factor.

III. Numerical Results

Several reasons led us to simulate the activity of the human FDI: it is a muscle without agonist, with pennation angle 0 and well documented in the literature [3, 4, 15].

The 267 MUs were positioned within the circular MCSA of the FDI using algorithms 1 and 2. The latter provided better results than the first. The global fiber density within the MCSA varies more when computed with algorithm 1 than with algorithm 2 (Fig. 3 and 4). Although the MUT centers were positioned mainly in a deterministic way (when the major parts of the MCSA were covered with at least one MUT, usually only a set of one point resulted in the smallest variance), the distribution of the MUT centers was compatible ($\div^2$-test) with an homogenous distribution (Fig. 5). We can conclude that algorithm 2 yields a relatively constant fiber density as found in real human muscles.

In the first simulation of the surface EMG, 20 electrodes were positioned around the muscle in the plane located 10 mm above the motor endplates. The distance between the surface of the muscle and the electrodes was 2 mm (corresponding to a skin thickness of 2 mm), and the radial angle between consecutive electrodes was 18° (corresponding to 3.86 mm). The difference between two neighboring electrodes was determined as for the usual bipolar recordings used in human subjects. The muscle was activated at a nearly constant level (activation factor at about 1.7, [3]).

On Fig. 6, the 20 EMGs are shown for 20 ms in the same sequence as they are arranged around the muscle. In this way, one can observe how MUAPs vary in time and as a function of the recording position around the muscle. Looking at EMGs as a function of time, it can be seen that most MUAPs have a triphasic shape corresponding to the 3 current sources and sinks passing at the recording electrodes. Their duration

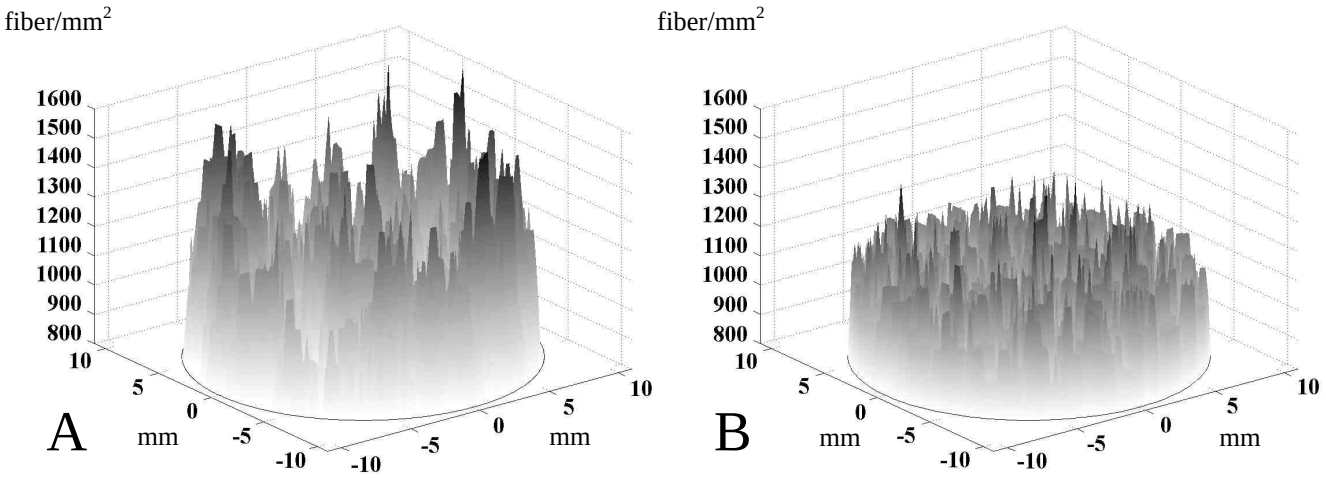

Fig. 4. Global fiber density of the FDI muscle in the circular MCSA resulting from algorithm 1 (A) and 2 (B). The peaks in A are of higher amplitude than in B.

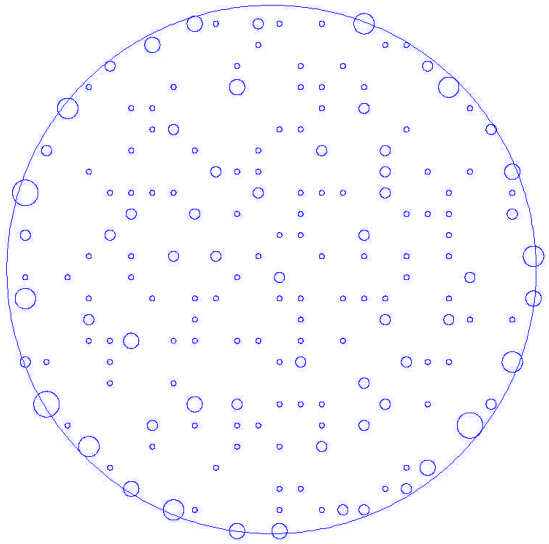

Fig. 5. MUT positions given by algorithm 2 described in the text. The size of a circle is increased with the number of circles at the same location. Superposition of centers is due to discretization process.

corresponds to the time of generation at the motor endplate till their disappearance at both muscle ends. Their size is mainly determined by the MU size and the distance of the MUT from the recording electrodes. Looking at the EMGs as a function of location, a MUAP can best be recorded by a particular electrode pair. They decrease in size with neighboring electrodes. The decrease is MU dependent and presumably faster the smaller the MU and the closer to the recording electrodes the MU is located. Each AP of a MU generates a particular hill on the *x*-*y* plane of Fig. 6. This feature might be the key for algorithms, which can separate the activity of individual MUs on the basis of multiple surface EMG recordings.

In the second simulation of the surface EMG, 14 surface electrodes (also 2 mm from the muscle surface) were placed longitudinally 26 mm along the muscle starting at the level of the motor endplate. The inter-electrode distance is thus 2 mm and the last electrode extends 6 mm over the muscle end. Again bipolar recordings were computed, as difference between a more distal and a more proximal EMG. The muscle was activated in the same way as in the first simulation. In Fig. 7, the 13 surface EMGs are presented during 9 ms as function of the position of the middle between the 2 recording electrodes. Mainly a positive peak of the MUAP is visible on Fig. 7, whereas negative peaks are partly hidden. The two tripoles generated at the motor endplate interact and generate a relatively small MUAP at the first electrode pair and the largest at the second pair. Further along the muscle, the MUAP is mainly influenced by the tripole below the electrodes and remains thus of constant size. Around the beginning of the linear decrease of the tripoles at 18 mm, the MUAP decreases in size till it disappears at the last recording site.

IV. Discussion

The basic approach for the computation of the surface EMGs has been developed since a long time [13]. However, the simulation of the 3-dimensional structure of a muscle, the simulation of its activity, including the recruitment order and the MU rate modulation, and the simulation of the surface EMG have never been achieved simultaneously. The major problems about the structure of a muscle was to find all the data required for a realistic reconstruction and to position the MUTs within the MCSA. The simulations presented in

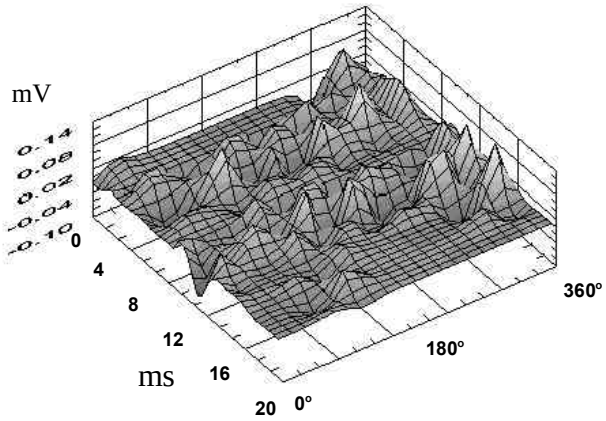

Fig. 6. Twenty simulated bipolar surface EMGs. The electrodes are positioned at equal distance around the muscle 10 mm above the motor endplates. Each EMG corresponds to the difference between two neighboring electrodes. *X*-axis: angular position of the EMGs around the muscle (degrees), *y*-axis: time (ms), *z*-axis: EMG (mV). Several MUs are active. Each MU generates a specific hill within the surface.

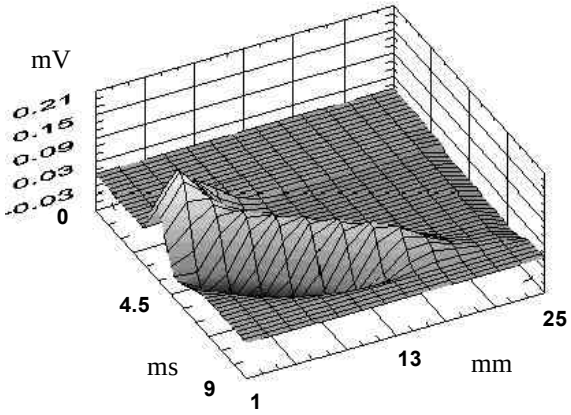

Fig. 7: Thirteen simulated bipolar surface EMGs. The electrodes are positioned at equal distance (2 mm) along the muscle, starting at the level of the motor endplates. Each EMG corresponds to the difference between two neighboring electrodes (distal minus proximal). *X*-axis: longitudinal position of the center of the two electrodes of an EMG starting at the motor endplates (mm); *y*-axis: time (ms); *z*-axis: EMG (mV). Only one MU is active.

Numerical Results have shown that the features of multiple surface EMGs, as found with recordings from human subjects, can be reproduced with the model. Emphasis is not put on the shape of individual MUAPs, there is no one-to-one relation between the MUs of a real and a simulated muscle, but we are interested in the behavior of the whole MU population within an active muscle.

All the present simulations have been performed in reasonable computing time with a LabView program on a PC. The most time-consuming procedure was the positioning of the MUTs in the MCSA. Fortunately this operation has to be performed only once for a particular muscle. In addition, for both configurations, the MUAPs of all MUs at all electrodes were computed in advance for later retrieval for the EMG simulation itself. In this way, surface EMGs of a muscle, in which up to 267 MUs can be active, could be performed on the present system with a time resolution of 0.1 ms.

Care was taken to maintain a modular design of the simulation of the whole motoneuronal pool-muscle complex whose major parts are (1) the input system to the motoneuronal pool, (2) the motoneuronal pool, (3) the force generating mechanism, (4) the 3-dimensional muscle model and (5) the simulation of the surface EMG. As already exemplified for module (4) and (5), results from individual modules can be saved and used for analysis or as input for other modules.

V. Conclusion

The present two modules of the simulation of the motoneuronal pool-muscle simulation are the last two to be developed. The generality of the system enables to simulate activation patterns of a variety of human muscles as they occur during normal motor behavior. It will be of special interest to investigate monosynaptic reflexes in the soleus muscle, which is very special in the sense that it has a pennation angle of 30° and very short fibers compared to its length. A further field of interest is to develop algorithms to separate the activity of single MUs from multiple surface recordings. With such a model, technical problems concerned with the recording of multiple surface EMGs can be differentiated from computational problems with separation of multiple MUAPs on the recordings.

References

[1] E. Henneman, “Principles governing distribution of sensory input to motor neurons,” in *The Neurosciences, 3 rd Study Program,* F.O. Schmitt, F.G. Worden (eds), Cambridge, MIT Press, 1974, pp. 281-291.

[2] J.E. Desmedt, “Size principle of motoneuron recruitment and the calibration of muscle force and speed in man,” in *Motor Control Mechanismus in Health and Disease*, J.E: Desmedt, New York: Raven Press, 1983, pp. 227-251.

[3] R. Nussbaumer, “Computer simulation of the motoneuron pool-muscle complex”, Doctoral Thesis, Fribourg, 2001.

[4] L.M. Studer, D.G. Ruegg, and J.-P. Gabriel, “A model for steady isometric muscle activation,” *Biol. Cybern.,* vol. 80, pp. 339-355, 1999.

[5] M.A. Johnson, J. Polgar, D. Weightman, and D. Appleton, “Data on the distribution of fibre types in thirty-six human muscles. An autopsy study,” *J. Neurol. Sci.,* vol. 18(1), pp. 111-29, January 1973.

[6] J. Polgar, M.A. Johnson, D. Weightman, and D. Appleton, “Data on fibre size in thirty-six human muscles. An autopsy study,” *J. Neurol. Sci.,* vol. 19, pp. 307-318, 1973.

[7] S. Bodine-Fowler, A. Garfinkel, R.R. Roy, and V.R. Edgerton, “Spatial distribution of muscle fibers within the territory of a motor unit,” *Muscle Nerve,* vol. 13(12), pp. 1133-45, December 1990.

[8] R.E. Burke, and P. Tsairis, “Anatomy and innervation ratios in motor units of cat gastrocnemius” *J. Physiol.,* vol. 234, pp. 749-765, 1973.

[9] R.R. Roy, A. Garfinkel, M. Ounjian, J. Payne, A. Hirahara, E. Hsu, and V.R. Edgerton, “Three-dimensional structure of cat tibialis anterior motor units,” *Muscle Nerve,* vol. 18, pp. 1187-95, October 1995.

[10] E. Eldred, A. Garfinkel, E.S. Hsu, M. Ounjian, R.R. Roy, and V.R. Edgerton, “The physiological cross-sectional area of motor units in the cat tibialis anterior,” *Anat. Rec.,* vol. 235(3), pp. 381-9, March 1993.

[11] S.C. Bodine, R.R: Roy, E. Eldred, and V.R. Edgerton, “Maximal Force as a Function of Anatomical Features of Motor Units in the cat tibialis anterior”, *J Neurophysiol*, vol. 57, pp. 1730-1745, June 1987.

[12] L.A. Geddes, and L.E. Baker, “The relationship between input impedance and electrode area in recording the Ecg,” *Med. Biol. Eng.* vol. 4(5), pp. 439-50, September 1966.

[13] S. Andreasson, and A. Rosenfalck, “Relationship of intracellular and extracellular action potentials of skeletal muscle fibers,” *CRC Crit. Rev. Bioeng.*, vol 6(4), pp. 267-306, November 1981.

[14] H. Reucher, J. Silny, and G. Rau, “Spatial filtering of noninvasive multielectrode EMG: Part II--Filter performance in theory and modelling,” *IEEE Trans. Biomed. Eng.,* vol. 34(2), pp.106-13, February 1967.

[15] H.S. Milner-Brown, R.B. Stein, and R. Yemm, “The contractile properties of human motor units during voluntary isometric contractions,” *J. Physiol. Lond.,* vol. 228, pp. 185-306, 1973.